Respiratory Research

RESEARCH

Open Access

Lsm2 is critical to club cell proliferation and its inhibition aggravates COPD progression

Wensi Zhu[1,7,8†], Linxiao Han[1,7,8†], Ludan He[2,7,8†], Wenjun Peng[1,7,8†], Ying Li[5†], Weibin Tian[3†], Hui Qi[6], Shuoyan Wei[1,7,8], Jie Shen[9], Yuanlin Song[2,8], Yao Shen[3*], Qiaoliang Zhu[4*] and Jian Zhou[1,2,7,8,9*]

Abstract

Background Chronic obstructive pulmonary disease (COPD) is a prevalent respiratory condition, with its severity inversely related to the levels of Club cell 10 kDa secretory protein (CC10). The gene *Lsm2*, involved in RNA metabolism and cell proliferation, has an unclear role in COPD development.

Methods An in vitro COPD model was developed by stimulating 16HBE cells with cigarette smoke extract (CSE). To establish an in vivo COPD model, mice with defective Lsm2 gene expression in lung or club cells were exposed to cigarette smoke for 3 months. Multiplexed immunohistochemistry (mIHC) was employed to identify the specific cells where Lsm2 gene expression is predominant. RNA sequencing and single-nucleus RNA sequencing were conducted to investigate the role of Lsm2 in the pathogenesis of COPD.

Results In this study, we found that cigarette smoke extract increases Lsm2 expression, and knocking down Lsm2 in 16HBE cells significantly reduces cell viability in vitro. mIHC showed that Lsm2 is primarily expressed in Club cells. Knockout of *Lsm2*, either in the lungs or specifically in Club cells, exacerbated lung injury and inflammation caused by cigarette smoke exposure in vivo. Single-nucleus RNA sequencing analysis revealed that Club cell-specific knockout of *Lsm2* leads to a reduction in the Club cell population, particularly those expressing $Chia1^{+}/Crb1^{+}$. This decrease in Club cells subsequently reduces the number of ciliated epithelial cells.

Conclusion Knocking out *Lsm2* in Club cells results in a significant decrease in Club cell numbers, which subsequently leads to a reduction in ciliated epithelial cells. This increased lung vulnerability to cigarette smoke and accelerating the progression of COPD. Our findings highlight that Lsm2 is critical to club cell proliferation and its inhibition aggravates COPD progression.

Keywords Lsm2, COPD, Club cells, Ciliated epithelial cells

†Wensi Zhu, Linxiao Han, Ludan He, Wenjun Peng, Ying Li and Weibin Tian contributed equally to this work.

*Correspondence:
Yao Shen
13611692261@163.com
Qiaoliang Zhu
zhuqiaoliang111@126.com
Jian Zhou
zhou.jian@fudan.edu.cn
[1] Department of Pulmonary and Critical Care Medicine, Shanghai Respiratory Research Institute, Zhongshan Hospital, Fudan University, 180 Fenglin Rd, Shanghai 200032, China
[2] Shanghai Institute of Infectious Disease and Biosecurity, Fudan University, Shanghai 200032, China
[3] Department of Respiratory and Critial Care Medicine, Shanghai Pudong Hospital, 2800 Gongwei Rd, Shanghai 201399, China
[4] Department of Thoracic Surgery, Shanghai Geriatric Medical Center, 2560 Chunshen Road, Shanghai 201104, China
[5] Department of Respiratory Endoscopy, Shanghai Chest Hospital, Shanghai Jiao Tong University, Shanghai 200030, China
[6] Hebei Academy of Integrated Traditional Chinese and Western Medicine, Shijiazhuang 050091, Hebei, China
[7] Shanghai Engineering Research Center of Internet of Things for Respiratory Medicine, 180 Fenglin Road, Shanghai 200032, China
[8] Shanghai Key Laboratory of Lung Inflammation and Injury, 180 Fenglin Road, Shanghai 200032, China
[9] Center of Emergency and Critical Medicine in Jinshan Hospital of Fudan University, Fudan University, Shanghai 200540, China

Introduction

Chronic obstructive pulmonary disease (COPD) is a heterogeneous lung disorder characterized by persistent respiratory symptoms such as dyspnea, cough, and expectoration. These symptoms result from ongoing, often progressive, airflow obstruction due to irregularities in the airways (bronchitis, bronchiolitis) or alveoli (emphysema) [1]. The pathogenesis of COPD involves complex interactions between genetic predispositions and environmental factors, significantly influencing susceptibility to the disease and its progression over an individual's lifetime [2].

The airway epithelium comprises multiple cell types, predominantly ciliated, goblet, basal, and Club cells [3]. Club cells, identified by the marker Scgb1a1^{+}, are non-ciliated secretory cells found in the bronchioles and trachea [4]. These cells have self-renewal ability and play a crucial role in airway tract repair, secreting anti-inflammatory and immunomodulatory proteins [5]. In COPD, cigarette smoke (CS) damages Club cells, leading to decreased secretion of the protein CC10 into circulation [6, 7]. Previous studies have shown that CC10 levels are negatively correlated with the severity of COPD and are associated with the airflow limitation index [6, 7].

Ciliated epithelial cells, which constitute at least 50% of airway epithelial cells, are the predominant epithelial cell type [8]. Their primary function is to facilitate the clearance of airway mucus [9]. In COPD patients, structural changes occur in ciliated epithelial cells, including shortened cilia and reduced ciliary beating frequency [10, 11]. Cilia dysfunction can exacerbate COPD symptoms; however, the mechanisms underlying this dysfunction remain unclear.

LSM2 belongs to the extensive family of Sm-like proteins (LSM), which are highly conserved across species and play crucial roles in RNA metabolism signaling pathways [12]. Previous studies have shown that the LSM1-7 complex, localized in the cytoplasm and interacting with decapping enzymes, enhances mRNA sensitivity to the 5′ to 3′ exonuclease enzyme XRN-1 [13]. In contrast, the LSM2-8 complex resides in the nucleus and comprises the U6 small nuclear ribonucleoprotein. LSM2 specifically recognizes the 3' end sequence of U6 RNA, facilitating interactions with other splicing factors to catalyze RNA splicing and regulate gene expression [14]. mRNA splicing is essential for generating protein diversity and maintaining biological homeostasis. Several studies have linked elevated LSM2 expression to the onset and prognosis of cancers, including ovarian, breast, liver, and lung cancers [15–18]. However, the role of LSM2 in COPD remains unclear.

In this study, we investigated the role of Lsm2 in COPD pathogenesis, identifying its significant impact on the number of ciliated epithelial cells by influencing Club cell proliferation. Our findings offer novel insights into COPD treatment.

Material and methods

Sex as a biological variable

Our study examined male and female animals, and similar findings are reported for both sexes.

Bioinformatics analysis

The GSE5058 and GSE8545 datasets were selected from the GEO database (https://www.ncbi.nlm.nih.gov/geo/) to analyze LSM2 expression in lung tissue. Only non-smokers (Control) and COPD patients were included in both datasets. The following are the steps: (1) Data Retrieval and Download. Visit the GEO database (https://www.ncbi.nlm.nih.gov/geo/) and then download the series matrix file, which typically contains gene expression data and sample annotation information. (2) Load R packages. The R packages include limma for differential analysis, GEOquery for data acquisition and preliminary processing, and ggplot2 for visualization. (3) Data Preprocessing. Use GEOquery to read the downloaded data and convert it into an appropriate expression matrix and remove unnecessary annotation information, retaining only gene names and sample expression values. (4) Extraction of Target Gene Expression Data. From the preprocessed expression matrix, based on the gene ID, accurately screen out the ID_REF corresponding to the target gene (LSM2). (5) Visualization of Expression Levels. Use ggplot2 to draw a box plot of LSM2.

Construction of COPD model with lung-specific Lsm2 knockout mice

Eight-week-old C57BL/6 mice were purchased from Cyagen Bioscience Inc. (Suzhou, China) and intratracheally instilled with 50 μL of ADM-GFP, which were randomly divided into two groups: NC and NC_CS. C57BL/6J-Lsm2$^{em\#1(flox)Smoc}$ mice (targeted transcript (Ensembl number): Lsm2-201 (ENSMUST00000007266.13), Flox targets exons: exon3, 4, 5) were generated by the Shanghai Model Organisms Center, Inc. (Shanghai, China). To induce lung-specific Lsm2 knockout, 50 μL of AdV5-CMV-Cre-mCMV-copGFP was intratracheally instilled. Subsequently, lung-specific Lsm2 knockout (Lsm2$^{-/-}$) mice were randomly divided into two groups, Lsm2$^{-/-}$ and Lsm2$^{-/-}$_CS, each containing five mice. All mice were housed in the animal facility at Zhongshan Hospital Affiliated with Fudan University, maintained under suitable environmental conditions (temperature, humidity, 12-h light/dark cycle), and provided ad libitum access to food and water. Two weeks after intratracheal instillation, the WT_CS and Lsm2$^{-/-}$_CS groups were exposed to CS

for 3 months to establish a COPD model (5 days a week, 20 cigarettes per day, 6 h of exposure per day; Daqianmen, Shanghai, China).

Construction of COPD model with club cell-specific Lsm2 knockout mice

To generate Club cell-specific Lsm2 knockout mice ($Lsm2^{\Delta Scgb1a1}$), C57BL/6J-$Lsm2^{em\#1(flox)Smoc}$ mice were crossed with Scgb1a1-IRES-Cre mice obtained from the Shanghai Model Organisms Center, Inc. Wild-type control mice were 8-week-old male C57BL/6 mice purchased from Cyagen Bioscience Inc. and randomly assigned to WT and WT_CS groups. All mice were housed in the animal facility at Zhongshan Hospital Affiliated with Fudan University. Mice in the WT_CS and $Lsm2^{\Delta Scgb1a1}$_CS groups were exposed to CS for 3 months to establish a COPD model (5 days a week, 20 cigarettes per day, 6 h of exposure per day; Daqianmen, Shanghai, China).

Hematoxylin and eosin (HE) staining

After euthanizing the mice, the right upper lung was fixed in 10% formalin for at least 24 h. The tissue was then paraffin-embedded, and 3 μm sections were prepared. HE staining was performed following the manufacturer's instructions [19].

Multiplexed immunohistochemistry (mIHC)

Four-μm-thick lung tissue sections were dewaxed and stained using the TSA 7-color kit (abs50029-100T, Absinbio, Shanghai, China). Initially, sections were incubated overnight at 4 °C with a Foxj1 antibody (1:200, 14-9965-82, Invitrogen, Carlsbad, CA, USA). They were then treated with an anti-rabbit horseradish peroxidase-conjugated secondary antibody (abs50015-02, Absinbio, Shanghai, China) for 10 min. Labeling was conducted for 10 min using TSA 520 as per the manufacturer's instructions. Slides were washed with Tris Buffered Saline with Tween-20 (TBST) (PS103, Epizyme, Shanghai, China) and subjected to antigen retrieval in preheated citrate solution (90 °C), followed by cooling to 25 °C in citrate solution. Tris buffer was used for washing between each step. Sodium citrate was utilized for repair. The same process was repeated for subsequent antibodies and fluorescent dyes: anti-Scgb1a1/TSA 570 (1:200, MA5-29780, Thermo Fisher Scientific, Waltham, MA, USA), anti-Lsm2/TSA 620 (1:200, NBP2-38093, Novus, Littleton, CO, USA), and anti-Krt5/TSA700 (1:100, ab64081, Abcam, Cambridge, UK). Each slide was then treated with DAPI (abs47047616, Absinbio, Shanghai). Finally, images were captured using PhenoImager HT (Akoya Biosciences, USA) and analyzed with Halo software (Indica Labs, USA).

Image quantification and colocalization analysis was performed using ImageJ software (National Institutes of Health, USA). Briefly, each individual channel image was first converted into a stack. The Line Tool from the toolbar was then used to select the cell of interest. For the analysis, CC10 protein was localized to the cytoplasm, while FOXJ1 and LSM2 were localized to the nucleus. A line was drawn through the selected cell to ensure it traversed both cytoplasmic and nuclear regions. Finally, the variation in fluorescence intensity along the selected line was analyzed. During the counting of positive cells, the threshold for $FOXJ1^+$ cells was set to 33–255, for $LSM2^+$ cells to 50–255, for $CC10^+$ cells to 49–235, and for $KRT5^+$ cells to 38–255. To ensure accurate cell identification, size and circularity parameters were adjusted to include cells with the expected morphology (size range [8 μm^2–∞], circularity [0.3–1]). Only particles within the thresholded region and exhibiting fluorescence intensity above the set threshold were considered positive.

Immunohistochemistry (IHC)

Sections were dewaxed using xylene and subsequently treated with 100%, 90%, and 75% ethanol. They were then fixed with citrate and incubated overnight at 4 °C with an Lsm2 antibody (1:200, NBP2-38093, NOVUS). The following day, the sections were incubated with horseradish peroxidase-conjugated secondary antibodies for 60 min at room temperature. Subsequently, 3,3′-diaminobenzidine staining was performed, and the stained sections were observed under a microscope (Olympus, Tokyo, Japan) [20].

Enzyme-linked immunosorbent assay (ELISA)

Bronchoalveolar lavage fluid (BALF) was collected following established procedures outlined in the literature [21]. ELISA kits specific for IL-6 (DY406, R&D Systems, Minneapolis, MN, USA), CXCL15 (DY442, R&D Systems), and TNF-α (DY410, R&D Systems) were used to quantify their levels in the BALF samples.

Immunofluorescence (IF)

After dewaxing and fixing, 3 μm paraffin sections were stained with antibodies against acetylated α-tubulin (1:500, T7451, Sigma-Aldrich, Saint Louis, MO, USA). The sections were incubated overnight at 4 °C with the primary antibodies. Subsequently, the sections were incubated for 1 h at 37 °C with Alexa Fluor® 488 goat anti-mouse IgG (H+L) (A11001, Thermo Fisher Scientific). For nuclear counterstaining, 4′,6-diamidino-2-phenylindole (DAPI, C1006, Beyotime Biotechnology, Shanghai, China) was used.

Scanning electron microscopy (SEM) and transmission electron microscopy (TEM)

The mouse trachea was initially fixed with a solution containing 2.5% glutaraldehyde and 1.5% paraformaldehyde for 3 h at room temperature. Following this, the specimens were treated with 1% OsO_4 for 2 h at room temperature. After fixation, the specimens underwent dehydration using a series of graded ethanol solutions. They were then dried using a critical-point dryer (Quorum, K850, UK), mounted on stubs, and finally coated with gold–palladium using a cold sputter coater (HITACHI, MC1000, Tokyo, Japan). The prepared specimens were examined using a scanning electron microscope (SEM) (HITACHI, SU8100, Tokyo, Japan).

For TEM, tissue samples were embedded in araldite CY212 resin. The embedded samples were sectioned into 1 μm thick sections and stained with toluidine blue after dehydration to aid in locating regions of interest. Ultrathin sections (60–80 nm) were subsequently cut from the areas of interest, stained with uranyl acetate and alkaline lead citrate to enhance contrast, and examined using a Hitachi HT7700 electron microscope. This allowed for detailed analysis of the length and ultrastructure of cilia according to established methodologies documented in the literature [22].

RNA sequencing

The right mid-lung tissue from the mouse was obtained, and 1 mL of TRIzol (15596018CN, Thermo Fisher Scientific) was added to isolate the total RNA following the manufacturer's instructions. The purity and concentration of the extracted RNA were assessed using an ND-2000 spectrophotometer (NanoDrop Technologies, Thermo Fisher Scientific). To obtain high-quality RNA samples suitable for mRNA sequencing, Oligo (dT) magnetic beads were employed to enrich mRNA. The mRNA was then fragmented and reverse transcribed to synthesize complementary DNA (cDNA), which was ligated with adapters for sequencing purposes. Sequencing was conducted on the NovaSeq X Plus platform (PE150) (Illumina, San Diego, CA, USA) using the NovaSeq Reagent Kit. All experimental procedures and analyses were conducted at Majorbio Bio-pharm Biotechnology Co., Ltd. (Shanghai, China).

10X genomics single nucleus RNA sequencing

Whole lung tissue from the mice was initially minced and snap-frozen in liquid nitrogen for at least 2 h. The tissue was then dissociated using the Chromium Nuclei Isolation Kit (PN-1000494, 10× Genomics, Pleasanton, CA, USA) following the manufacturer's protocol for single nucleus RNA sequencing. To ensure high cell viability, cell suspensions were enriched using the Dead Cell Removal Kit (130-090-101, Miltenyi Biotec, Cologne, Germany), resulting in a concentration of 700–1200 cells/μL with a viability of ≥ 85%. These viable cells were then loaded on the 10× Genomics Chromium platform, with 10,000 cells used to prepare scRNA-seq libraries. The Chromium Single Cell 3′ Library and Gel Bead Kit V3.1 (PN1000268, 10× Genomics) was employed to generate single-cell gel beads in emulsion (GEM). After thorough quality control of the prepared libraries, sequencing was performed on an Illumina Novaseq 6000 platform using a 150 bp paired-end sequencing strategy at Berry Genomics Corporation (Beijing, China).

Cell culture and cigarette smoke extract (CSE) stimulation

16HBE cells were cultured in RPMI 1640 medium (Gibco, Carlsbad, CA, USA) supplemented with 10% fetal bovine serum (FBS, Gibco) and 1% penicillin–streptomycin (Gibco). They were incubated in a 37 °C incubator with 5% CO_2. When the cells reached suitable confluence, they were dissociated with trypsin (Gibco) and seeded into six-well plates. After 24 h of incubation, they were stimulated with 0.5%, 1%, or 1.5% CSE, or with 1.5% CSE for 24, 48, and 72 h. The extraction method of CSE is described in our previous studies [20].

Lentiviral infection and cell viability detection

Lentivirus-containing short hairpin RNA (shRNA) targeting Lsm2 and lentivirus vectors were obtained from Genechem (Shanghai, China). Appropriate concentrations of 16HBE cells were seeded into six-well plates and incubated in a 37 °C, 5% CO_2 incubator for 24 h. Once the cells reached 50–60% confluence, the medium was replaced with 1 mL of medium containing 5 μg/mL polybrene (Genechem), along with either lentivirus-containing shRNA targeting Lsm2 (shLsm2) or lentivirus vectors (negative control, NC). The cells were then incubated for 48 h. Following incubation, cells from the NC and shLsm2 groups were dissociated to obtain a cell suspension. Approximately 1×10^4 cells from each group were seeded in a 96-well plate and further incubated in a 37 °C, 5% CO_2 incubator for 48 h. Next, the medium was replaced with fresh culture medium containing 10% CCK-8 (SB-CCK8, SanegeneBio, Shanghai, China), and the cells were incubated for 1 h. Subsequently, the absorbance at a wavelength of 450 nm was measured to assess cell viability.

Quantitative real-time polymerase chain reaction (qRT-PCR)

RNA extraction from lung tissue was carried out using the RNA-Quick Purification Kit (RN001, Shanghai Yishan Biotechnology Co. Ltd., Shanghai, China). The extracted RNA was then reverse-transcribed into cDNA

Table 1 Primers used for quantitative real-time PCR

Gene	Sequence (5′→3′)
Mouse Lsm2 Forward	ACCCTGAGAAATACCCTCACAT
Mouse Lsm2 Reverse	GACGACTGAGCCCCTGATG
Human LSM2 Forward	CATCTGTGGAACCCTCCATTC
Human LSM2 Reverse	GCACGTATCGGACCACTGAG

using the PrimeScript™ RT reagent kit (RR037A, Takara Biotechnology, Osaka, Japan). qRT-PCR was performed to amplify the target genes using RR420A from Takara Biotechnology. The primer sequences are shown in Table 1.

Cell cycle detection

16HBE cells (2×10^5) from the shLsm2 or negative control (NC) group were seeded into 6-well culture plates and incubated at 37 °C in a 5% CO_2 incubator for 24 h. Once the cell density reached 80%, cells were digested with 0.25% trypsin (without EDTA) and collected into flow cytometry tubes. After centrifugation at 1500 rpm for 5 min, the cell pellet was resuspended in 300 µL PBS, and 700 µL pre-cooled anhydrous ethanol was slowly added dropwise while the tube was stored at −4 °C for overnight fixation. The following day, the fixed cells were mixed, and 3 mL PBS was added to each tube for resuspension. Cells were centrifuged again at 1800 rpm for 5 min, and the supernatant was discarded. Next, 10 µL of RNase (10 µg/mL) and 100 µL PBS were added to each tube, followed by incubation in a 37 °C water bath for 30 min. Finally, 20 µL propidium iodide (PI, 250 µg/mL) was added for resuspension, and the samples were prepared for analysis using the 70-CCS012 Cell Cycle Staining Kit (MultiSciences, China).

Statistical analysis

GraphPad Prism9.0 software was used for all data analyses. For normally distributed data, comparisons were made using the t-test and one-way analysis of variance (ANOVA) with Tukey's multiple comparison test. For non-normally distributed data, the Mann–Whitney U test was applied. Results are presented as the mean ± standard deviation (SD), with statistical significance defined as $p < 0.05$.

Results

Cigarette smoke enhances Lsm2 expression

In the GEO database, we compared the expression levels of LSM2 in lung tissue samples from healthy individuals and COPD patients. The results showed that LSM2 expression was significantly higher in the lung tissue of COPD patients compared to healthy individuals (Fig. 1A). We then compared *Lsm2* gene expression between wild-type (WT) mice and mice exposed to cigarette smoke for 3 months (Fig. 1B). The results showed increased Lsm2 expression in the WT_CS group at both the protein and gene levels (Fig. 1C, D). Additionally, LSM2 was visually confirmed to be expressed in airway epithelial cells, as shown in Fig. 1C. Thus, 16HBE cells stimulated with cigarette smoke extract (CSE) exhibited a concentration- and time-dependent increase in *Lsm2* gene expression, with the highest elevation observed after 1.5% CSE stimulation for 72 h (Fig. 1E–G). Knockdown of Lsm2 in 16HBE cells significantly reduced cell viability (Fig. 1H, I). Furthermore, compared to the NC group, the shLsm2 group exhibited significant changes in the cell cycle, with an increased proportion of cells in the S phase (Fig. 1J). These findings suggest that Lsm2 plays a crucial role in COPD development.

Lung-specific Lsm2 knockout exacerbates lung injury and inflammation induced by cigarette smoke exposure

To investigate Lsm2's role in COPD, we developed a conditional Lsm2 knockout mouse (C57BL/6J-Lsm2$^{em\#1(flox)Smoc}$). Lung-specific Lsm2 knockout (Lsm2$^{-/-}$) mice were generated by administering AdV5-CMV-Cre-mCMV-copGFP via intratracheal administration to C57BL/6J-Lsm2$^{em\#1(flox)Smoc}$ mice. These Lsm2$^{-/-}$ mice were exposed to CS for 3 months to establish a COPD model (Fig. 2A, B). Histological examination using HE staining revealed significant lung pathology in NC_CS mice, including prominent leukocyte infiltration, erythrocyte exudation, airway thickening (Fig. 2C). Lung-specific Lsm2 knockout mice exposed to CS (Lsm2$^{-/-}$_CS) exhibited even greater lung inflammation and injury, as evaluated by lung injury score, and mean alveolar septal thickness (MAST) [19, 23] (Fig. 2D).

We quantified TNF-α, CXCL15, and IL-6 levels in bronchoalveolar lavage fluid (BALF) using ELISA. The WT_CS group showed a significant increase in TNF-α, CXCL15, and IL-6 levels following CS exposure compared to the WT group. The Lsm2 knockout resulted in an even more pronounced elevation in TNF-α, CXCL15, and IL-6 secretion caused by CS (Fig. 2E).

Club cell-specific Lsm2 knockout exacerbates CS-induced lung injury

To determine the cell types where Lsm2 is mainly expressed, mIHC was used to stain LSM2 along with markers for epithelial cell types, specifically CC10$^+$ Club cells, FOXJ1$^+$ ciliated epithelial cells, and KRT5$^+$ basal cells (Fig. 3A and Supplementary Fig. 1A). LSM2 was primarily expressed in Club cells of wild-type mice (Fig. 3B, C and Supplementary Fig. 1B-C). Exposure to cigarette smoke increased the ratio of CC10$^+$LSM2$^+$/CC10$^+$cells

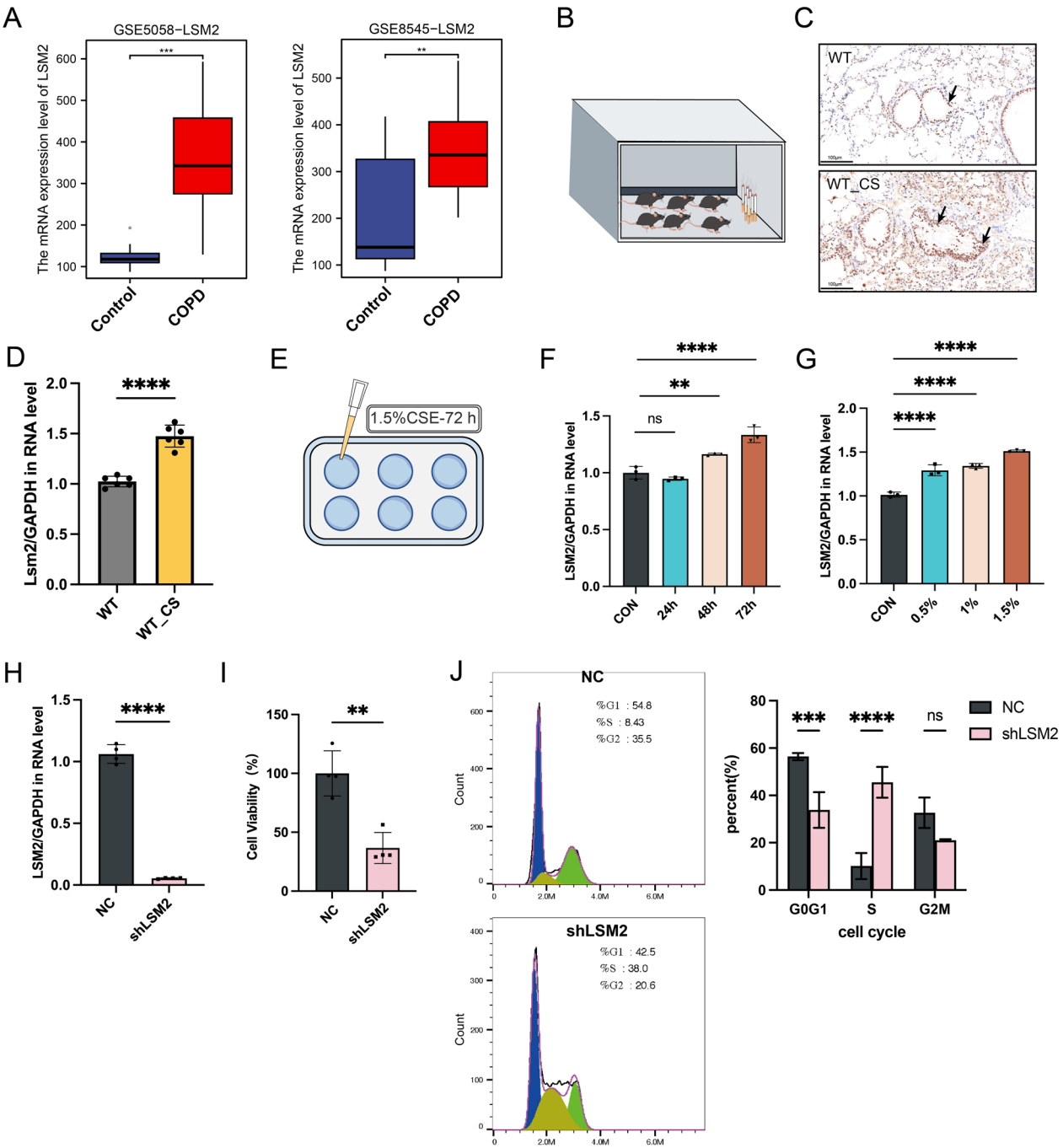

Fig. 1 Cigarette smoke enhances the expression of Lsm2. **A** The expression of LSM2 in nonsmokers (Control) and patients with COPD was obtained from the Gene Expression Omnibus (GEO) database, using datasets GSE5058 and GSE8545. **B** Schematic of COPD modeling. **C** Immunohistochemistry (IHC) of LSM2 (n = 3 biological replicates). Black arrows indicate LSM2^{+} cells. **D** Lsm2 gene expression in mice (n = 6 biological replicates). **E** Schematic diagram of CSE stimulation in 16HBE cells. **F** Expression of LSM2 in 16HBE cells stimulated with 1.5% CSE at different time points. **G** Expression of LSM2 in 16HBE cells stimulated with different concentrations of CSE for 72 h. **H** Lentivirus-containing short hairpin RNA (shRNA) targeting Lsm2 inhibited Lsm2 expression in 16HBE cells (n = 4 biological replicates). **I** Reduction in cell viability following Lsm2 knockdown (n = 4 biological replicates). **J** Cell cycle in NC and shLSM2 group (n = 3 biological replicates). $^{**}p < 0.01$; $^{****}p < 0.0001$

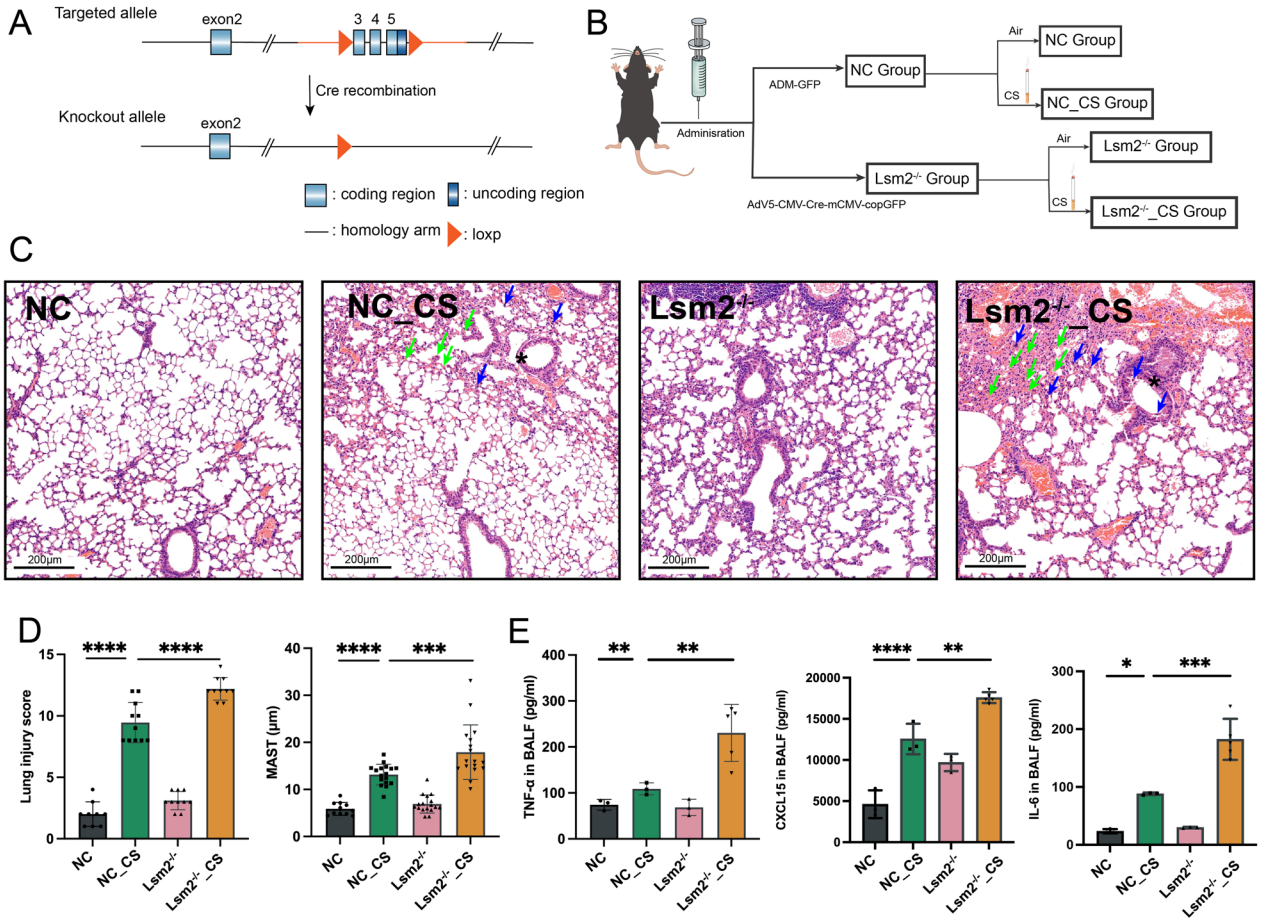

Fig. 2 Lung-specific Lsm2 knockout exacerbates cigarette smoke-induced lung injury and inflammation. **A** The diagram of design strategy for generating Lsm2 conditional knockout mice using CRISPR/Cas9 technique. **B** Experimental design schematic. **C** Hematoxylin and eosin (HE) staining. The green arrows point to exudative red blood cells, the blue arrows highlight infiltrating inflammatory cells, and the asterisk (*) denotes thickened airways. **D** Lung tissue pathology scoring, including lung injury score, and MAST, **E** concentration of TNF-α, CXCL15 and IL-6 in bronchoalveolar lavage fluid (BALF) (pg/mL); Values represent mean ± SD, n = 3–5 for each group. *p < 0.05; **p < 0.01; ****p < 0.0001. *NC group* Negative control mice, *NC_CS group* negative control mice exposed to cigarette smoke for 3 months, *Lsm2*$^{-/-}$ *group* lung-specific Lsm2 knockout mice, *Lsm2*$^{-/-}$*_CS group* Lung-specific Lsm2 knockout mice exposed to cigarette smoke for 3 months

(See figure on next page.)

Fig. 3 Club cell-specific Lsm2 knockout exacerbates cigarette smoke (CS)-induced lung injury. **A** Multiplexed immunohistochemistry (mIHC) of FOXJ1, CC10, and LSM2 (n = 3 biological replicates). **B** The percent of CC10^{+}LSM2^{+}/CC10^{+}Cells, FOXJ1^{+}LSM2^{+}/FOXJ1^{+}Cells, and CC10^{+}LSM2^{+}/Total cells (n = 3 biological replicates). **C** Fluorescence colocalization analysis. **D** Experimental design schema diagram. **E** Immunohistochemistry (IHC) staining of LSM2 and hematoxylin and eosin (HE) staining of lung tissue. **F** Lung tissue pathology scoring, including lung injury score, and MAST. The blue arrows indicate tar-engulfing macrophages, while the asterisk (*) marks the thinner airway epithelium in Lsm2$^{\Delta Scgb1a1}$ and Lsm2$^{\Delta Scgb1a1}$_CS groups compared to the WT and WT_CS groups. Values represent mean ± SD, n = 3–6 for each group. *p < 0.05; **p < 0.01; ****p < 0.0001

in the WT_CS group, indicating enhanced Lsm2 expression in Club cells following smoke exposure (Fig. 3B). This suggests that Lsm2 might play an important role in Club cells during COPD pathogenesis.

To investigate the role of Lsm2 in Club cells, we generated Club cell-specific Lsm2 knockout mice and exposed them to CS for 3 months (Fig. 3D). Immunohistochemical (IHC) staining of LSM2 confirmed the effectiveness of gene knockout, with negligible LSM2 protein expression in the lungs of Lsm2$^{\Delta Scgb1a1}$ and Lsm2$^{\Delta Scgb1a1}$_CS mice despite increased LSM2 expression following CS exposure (Fig. 3E).

HE staining showed notable disruption of lung tissue architecture in the WT_CS group, with the presence of

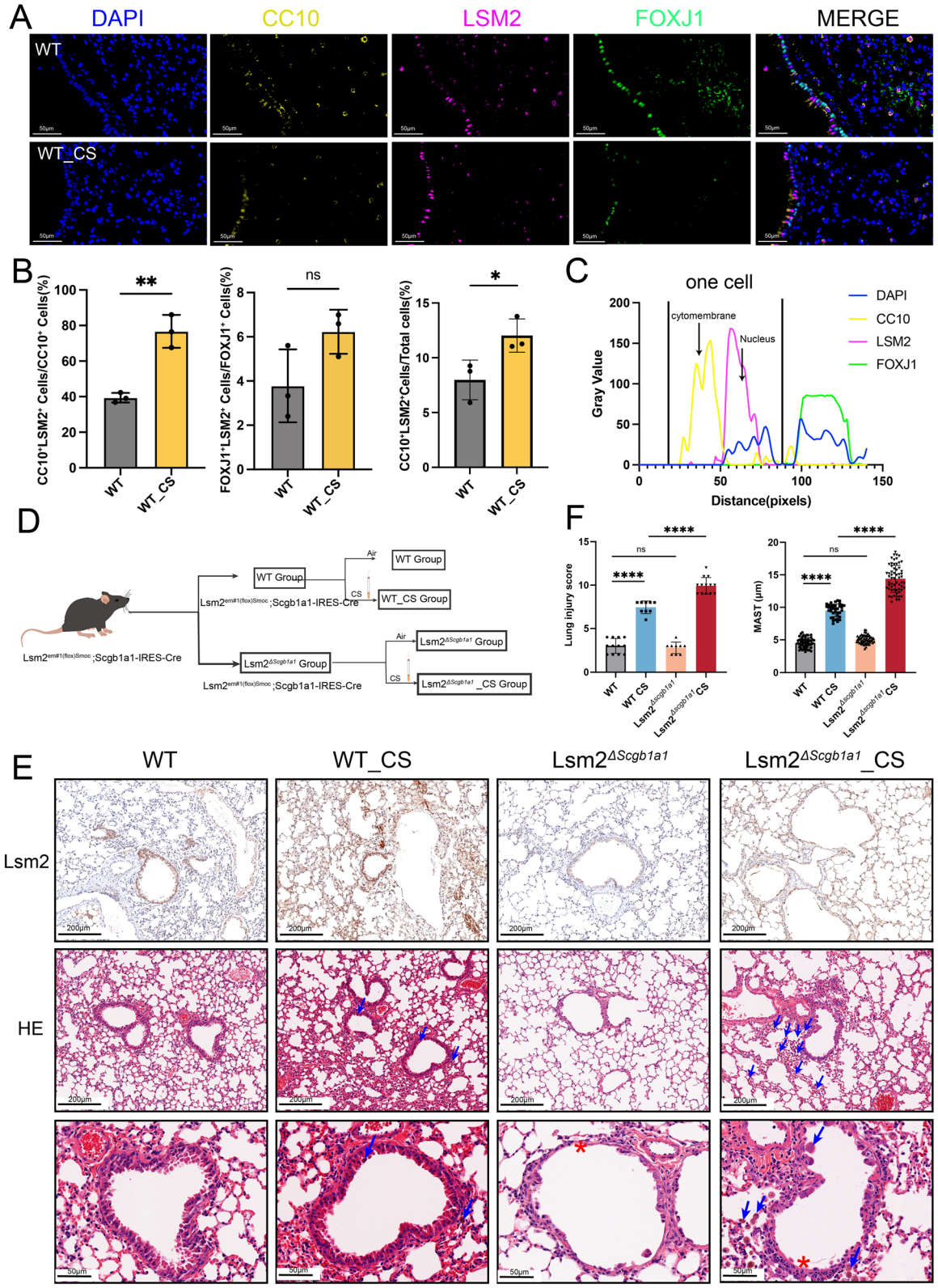

Fig. 3 (See legend on previous page.)

giant tar-devouring cells within the alveolar cavities along with inflammatory cell infiltration. The Lsm2$^{\Delta Scgb1a1}$_CS group exhibited more severe destruction, with increased infiltration of tar-engulfing macrophages (Fig. 3E). The airway epithelium in the Lsm2$^{\Delta Scgb1a1}$ and Lsm2$^{\Delta Scgb1a1}$_CS groups appeared thinner and more discontinuous than in the WT and WT_CS groups (Fig. 3E). However, compared with the WT group, the Lsm2$^{\Delta Scgb1a1}$ group did not have obvious inflammatory cell infiltration. Pathological scoring indicated that the lung injury score and MAST were significantly higher in the Lsm2$^{\Delta Scgb1a1}$_CS group compared to the WT_CS group (Fig. 3F). These results indicating that Club cell-specific Lsm2 knockout decreases the number of Club cells without inducing lung injury at baseline, but exacerbates CS-induced lung injury during CS exposure.

RNA-Seq analysis and inflammatory response

RNA-Seq analysis of lung tissues from the four groups of mice, and the differential expression of genes among these groups is depicted in Fig. 4A. Initially, we identified 306 genes with significantly increased expression following smoke exposure. Among these, 14 genes showed further increases upon Club cell-specific Lsm2 knockout (Fig. 4B, C). Gene Ontology (GO) enrichment analysis revealed significant involvement in immune response, innate immune response, and immune system processes, predominantly linked to inflammation (Fig. 4D).

To validate the RNA-Seq findings, we assessed inflammatory indicators by measuring white blood cell (WBC) count and IL-6, CXCL15, and TNF-α levels in BALF using ELISA. The WT_CS group showed significant increases in these markers compared to the WT group, with even higher levels in the Lsm2$^{\Delta Scgb1a1}$_CS group (Fig. 4E, F). Luminex assay confirmed increased secretion of IL-6, G-CSF, and MIP-1α in Club cell-specific Lsm2 knockout mice exposed to CS for 3 months, with similar trends observed for MCP-1, CXCL1, and IL-17A (Supplementary Fig. 2A). These results support the RNA-Seq data, emphasizing the role of LSM2 in regulating lung inflammation, particularly in Club cells, during COPD development.

Club cell-specific Lsm2 knockout induces ciliated epithelial cell defects

RNA-Seq analysis revealed that, compared to the WT_CS group, 573 genes exhibited decreased expression and 626 genes exhibited increased expression in the Lsm2$^{\Delta Scgb1a1}$_CS group (Fig. 4A and Supplementary Fig. 3A). To understand the functional implications of the downregulated genes in the Lsm2$^{\Delta Scgb1a1}$_CS group, we conducted GO functional enrichment analysis, which indicated a strong association with ciliated epithelial cell composition and function, including processes such as cilium movement, assembly, organization, and the structure of 9 + 2 motile cilium (Supplementary Fig. 3B). Subsequent qRT-PCR analysis confirmed that genes involved in these cilium-related pathways were significantly downregulated in the Lsm2$^{\Delta Scgb1a1}$_CS group compared to the WT_CS group (Supplementary Fig. 3C).

To further investigate the role of Club cell-specific Lsm2 knockout in ciliated epithelial cells, we examined cilia length and the "9 + 2" microscopic structure using electron microscopy and assessed ciliated epithelial cell beating frequency. Cigarette smoke exposure resulted in reduced cilia length in the WT_CS group, along with instances of ciliary membrane rupture, blistering, and dynein wall damage compared to the WT group (Fig. 5A, B).

The Lsm2$^{\Delta Scgb1a1}$_CS group showed significantly shorter cilia compared to the WT_CS group (Fig. 5B). However, there were no significant differences in the "9 + 2" structure between the Lsm2$^{\Delta Scgb1a1}$ and WT groups, or between the Lsm2$^{\Delta Scgb1a1}$_CS and WT_CS groups (Fig. 5A), suggesting that Club cell-specific Lsm2 knockout exacerbates cigarette smoke-induced cilia shortening but does not affect ciliary structure. Additionally, the WT_CS group exhibited decreased ciliary oscillation frequency compared to the WT group, indicating impaired ciliary function after cigarette smoke exposure (Fig. 5C). Club cell-specific Lsm2 knockout (Lsm2$^{\Delta Scgb1a1}$ and Lsm2$^{\Delta Scgb1a1}$_CS groups) did not alter ciliary oscillation frequency compared to the WT and WT_CS groups, respectively (Fig. 5C).

Using the ciliated epithelial cell marker α-tubulin, we observed a notable absence of α-tubulin^{+} cells within the airway epithelium of both the Lsm2$^{\Delta Scgb1a1}$ and Lsm2$^{\Delta Scgb1a1}$_CS groups compared to the WT and WT_CS groups (Fig. 5D, E). These findings indicate that Club cell-specific Lsm2 knockout reduces the number of ciliated epithelial cells.

Club cell-specific Lsm2 knockout modulates cellular composition

We conducted single-cell sequencing (10× Genomics) on lung tissue from four groups of mice to investigate the impact of Club cell-specific Lsm2 knockout on cellular composition. After FACS and quality control screening, we isolated 7889 cells from the WT group, 12,038 from the WT_CS group, 11,862 from the Lsm2$^{\Delta Scgb1a1}$ group, and 10,400 from the Lsm2$^{\Delta Scgb1a1}$_CS group (Fig. 6A).

Dimensionality reduction clustering analysis using t-distributed stochastic neighbor embedding (t-SNE) identified 29 cell types (Fig. 6B and Supplementary Fig. 5A), further categorized into 16 types based on marker gene expression levels (Fig. 6C). These

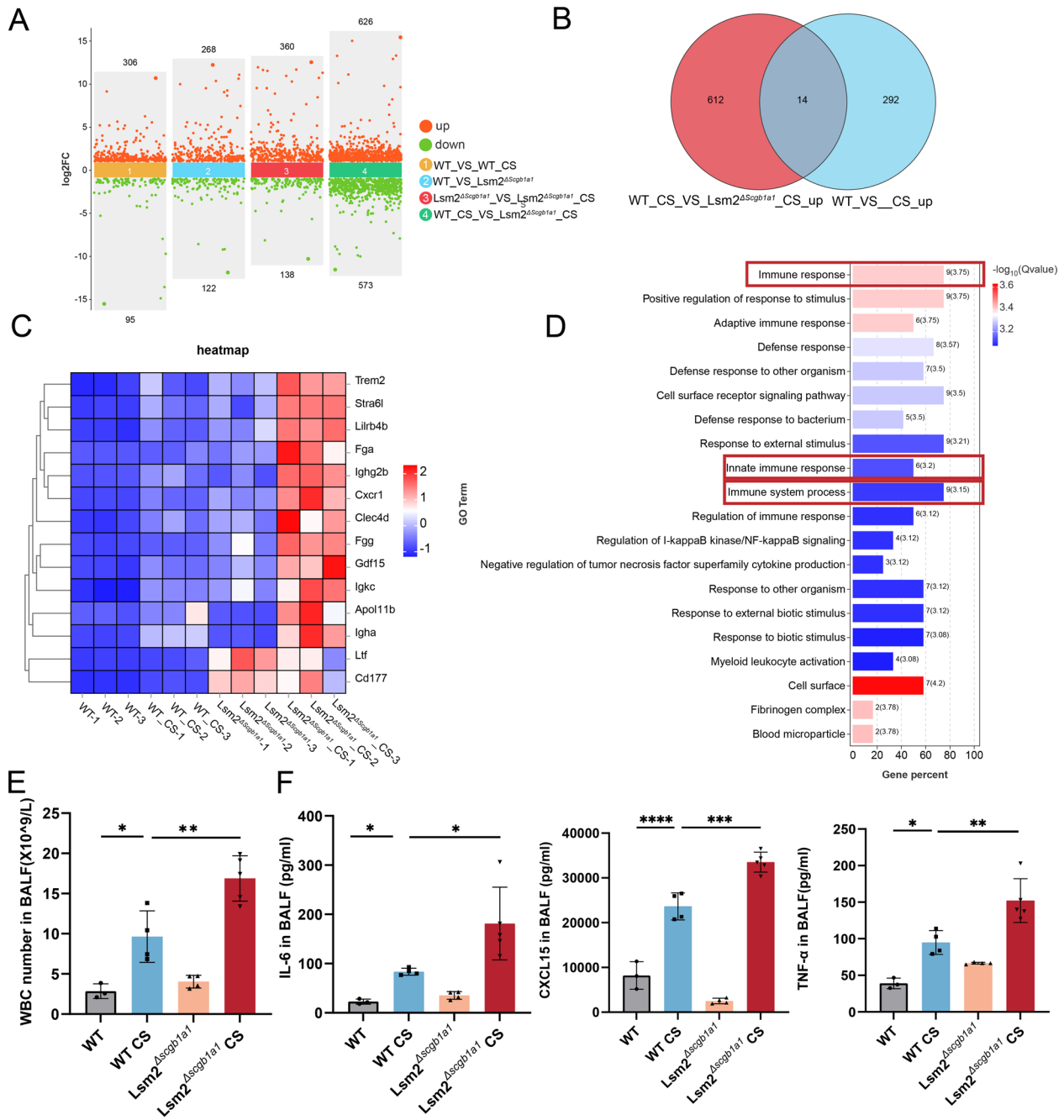

Fig. 4 Club cell-specific Lsm2 knockout exacerbates cigarette smoke (CS)-induced lung inflammation. **A** Number of differentially expressed genes in four groups (n = 3 biological replicates). **B**, **C** Differential genes with significantly increased expression following smoke exposure, which further increased upon Club cell-specific Lsm2 knockout. **D** Gene Ontology (GO) enrichment analysis of differentially expressed genes. **E** Number of white blood cells in bronchoalveolar lavage fluid (BALF). **F** Concentrations of IL-6, CXCL15, and TNF-α in BALF measured by ELISA (pg/ml). Values represent mean ± SD, n = 3–6 for each group. *p < 0.05; **p < 0.01; ***p < 0.001; ****p < 0.0001

included type II pneumocytes (Sftpc, Lamp3), macrophages (Mrc1), Club cells (Scgb1a1, Aldh1a1), lymphatic endothelial cells (Bmp6), type I pneumocytes (Ager, Akap5), B cells (Pax5, Bank1), T cells (Skap1, Itk), fibroblasts (Nox4, Pdgfra), monocytes (Adgre4, Ccr2), mesothelial cells (Upk3b), endothelial cells (Pecam1), ciliated epithelial cells (Cfap299, Dnah12), NK cells (Ncr1, Ccl5), pericytes (Pdgfrb), dendritic cells (Ccr7), and neuroendocrine cells (Bex2, Calca) (Fig. 6D).

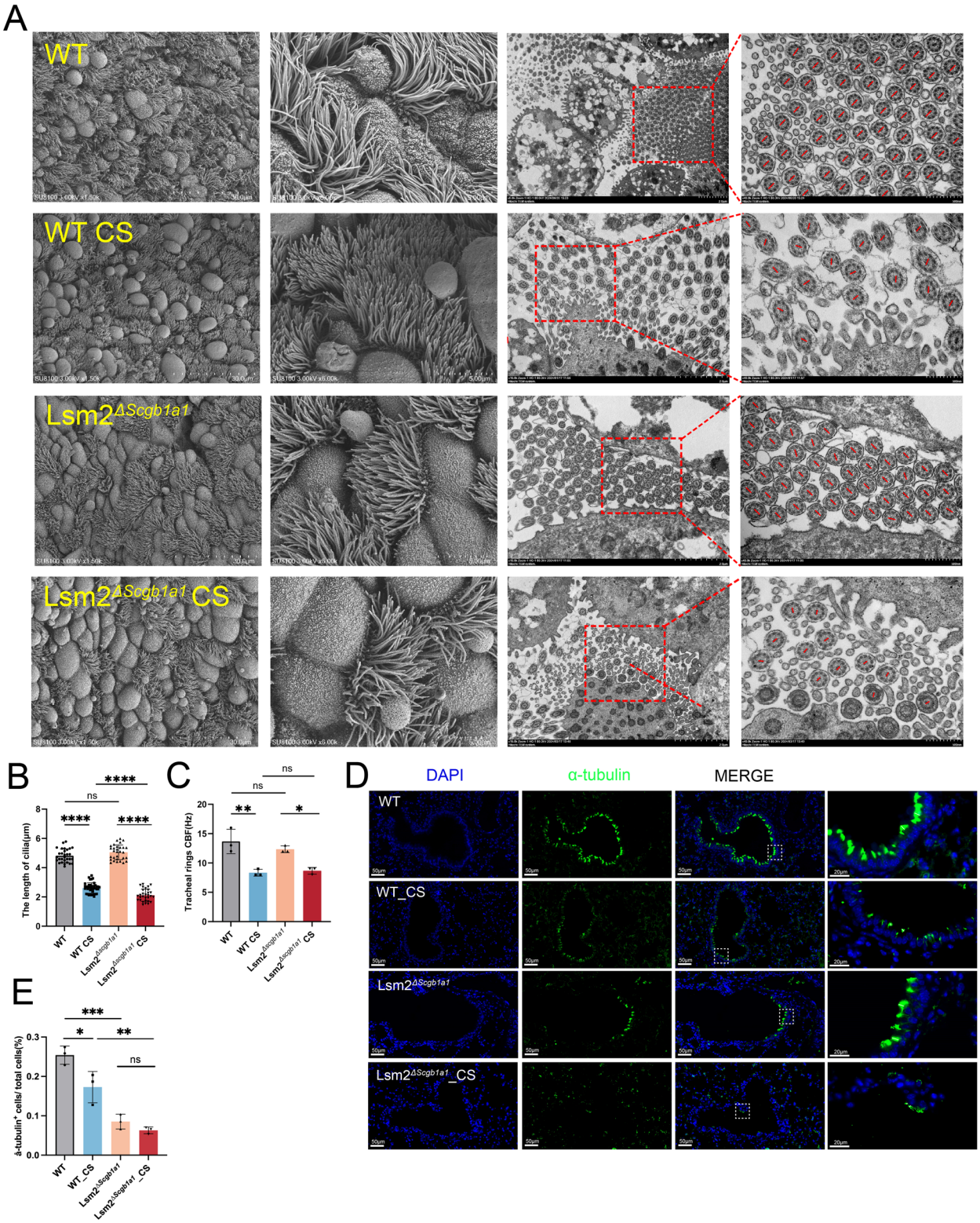

Fig. 5 Club cell-specific Lsm2 knockout decreases the number of ciliated epithelial cells. **A** Ciliary structure observed under scanning electron microscopy and transmission electron microscopy. **B** Length of cilia (μm). **C** Ciliary beat frequency (CBF, Hz) in tracheal rings. **D** Immunofluorescence (IF) of α-tubulin. **E** The percent of α-tubulin$^+$ cells. Values represent mean ± SD, n = 3 for each group. *p < 0.05; **p < 0.01; ***p < 0.001; ****p < 0.0001

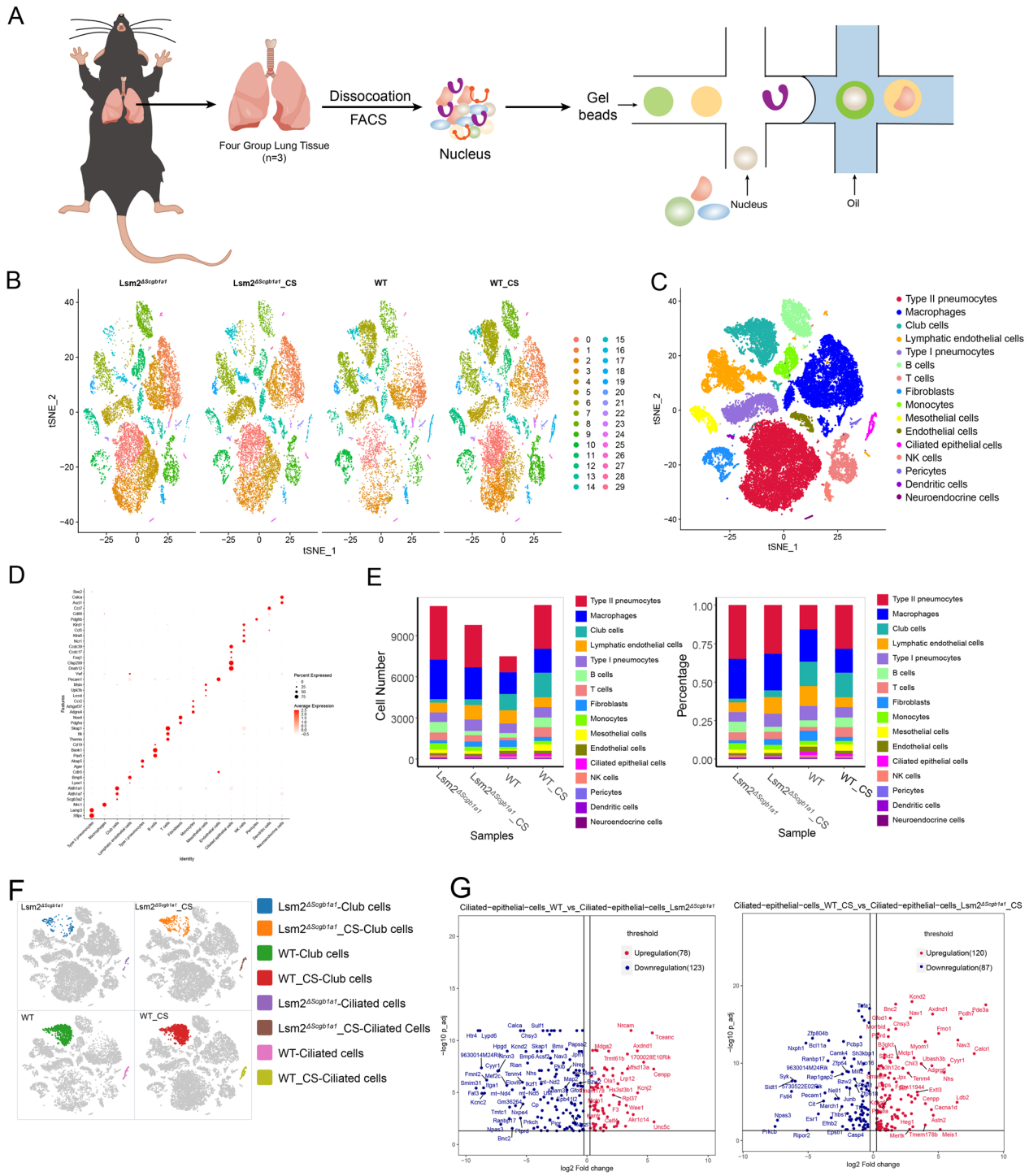

Fig. 6 Club cell-specific Lsm2 knockout modulates cellular composition. **A** Schematic of lung tissue dissociation to single-cell suspension and loading into the 10× Genomics System. **B** tSNE visualization of all lung cells showing 29 clusters and tSNE visualization of WT, WT_CS, Lsm2$^{\Delta Scgb1a1}$, and Lsm2$^{\Delta Scgb1a1}$_CS groups. **C** tSNE visualization profiling the major cell types. **D** Bubble plots of the marker genes expressed in the major cell types. **E** The number and percentage of the major cell types. **F** tSNE visualization of Club cells and ciliated epithelial cells in WT, WT_CS, Lsm2$^{\Delta Scgb1a1}$, and Lsm2$^{\Delta Scgb1a1}$_CS groups. **G** Volcano plot of differential genes of ciliated epithelial cells between WT and Lsm2$^{\Delta Scgb1a1}$ groups, and WT_CS and Lsm2$^{\Delta Scgb1a1}$_CS groups

Further investigation focused on changes in cell type numbers and proportions in each group. Cigarette smoke exposure increased both the number and proportion of Club cells from 1,191 (15.89%) in the WT group to 1,788 (15.94%) in the WT_CS group. In contrast, the $Lsm2^{\Delta Scgb1a1}$ group showed a significant decrease to 265 (2.38%). Although the number of Club cells slightly increased to 425 (4.35%) in the $Lsm2^{\Delta Scgb1a1}$_CS group compared to the $Lsm2^{\Delta Scgb1a1}$ group, it remained significantly lower than in the WT and WT_CS groups (Fig. 6E, F).

Significant changes were also observed in ciliated epithelial cells. Compared to the WT group (158, 2.11%), the proportion of ciliated epithelial cells in the WT_CS group decreased to 1.54% (173). The $Lsm2^{\Delta Scgb1a1}$ group showed a significant decrease to 31 (0.28%), while the $Lsm2^{\Delta Scgb1a1}$_CS group had 48 (0.49%) (Fig. 6E, F).

To minimize interference from immune cells, we selected $CD45^-$ cells and reclassified them into separate groups. The results showed that club cells comprise 23.34% in the WT group and 23.28% in the WT_CS group, whereas their proportions in the $Lsm2^{\Delta Scgb1a1}$ and $Lsm2^{\Delta Scgb1a1}$_CS groups are only 4.23% and 6.75%, respectively. Similarly, the proportions of ciliated epithelial cells in the four groups were as follows: WT group (3.1%), WT_CS group (2.25%), $Lsm2^{\Delta Scgb1a1}$ group (0.49%), and $Lsm2^{\Delta Scgb1a1}$_CS group (0.76%). Even after removing $CD45^+$ cells, we were still able to demonstrate that knockout of the Lsm2 gene in club cells significantly reduces the number of both club cells and ciliated epithelial cells (Supplementary Fig. 4).

Volcano plots depicting differential gene expression between the ciliated epithelial cells of WT and $Lsm2^{\Delta Scgb1a1}$ groups, as well as between the WT_CS and $Lsm2^{\Delta Scgb1a1}$_CS groups, are shown in Fig. 6G. GO enrichment analysis of differentially expressed genes from ciliated epithelial cells in the four groups revealed no association with cilia structure and function (Supplementary Fig. 5B, C). This further supports our conclusion that Club cell-specific Lsm2 knockout reduces the number of ciliated epithelial cells without affecting individual cilia function and structure.

Significance of $Chia1^+/Crb1^+$ club cells in transdifferentiation to ciliated epithelial cells

Club cell-specific Lsm2 knockout induces significant alterations in the airway epithelium of both the $Lsm2^{\Delta Scgb1a1}$ and $Lsm2^{\Delta Scgb1a1}$_CS groups. We re-clustered and analyzed airway epithelial cells from the four groups, resulting in 18 clusters (Fig. 7A, B). Among these, Club cells were subdivided into six distinct clusters, while ciliated epithelial cells comprised only one cluster (Fig. 7C). Previous studies have shown that Club cells can differentiate into ciliated epithelial cells, but the specific subtype crucial to this process remains unclear [24, 25]. To investigate the evolutionary dynamics between Club and ciliated epithelial cells, we conducted pseudo-time cell trajectory analysis of the six Club cell clusters and ciliated epithelial cells, revealing a three-branch trajectory illustrating the development from Club cells to ciliated epithelial cells (Fig. 7D).

After confirming the starting point, developmental routes were determined, bifurcating into either Cell fate 1 or Cell fate 2 branches. Significant differences emerged in Club cell cluster 7 between the Club cell-specific Lsm2 knockout and wild-type mice. Specifically, in the $Lsm2^{\Delta Scgb1a1}$ and $Lsm2^{\Delta Scgb1a1}$_CS groups, the number of Club cells in cluster 7 at the differentiation origin was notably reduced, with a higher proportion differentiating into Cell fate 2, a pattern absent in the WT and WT_CS groups. Club cell cluster 7 was identified as a subgroup characterized by $Chia1^+/Crb1^+$ cells (Fig. 7E). GO functional enrichment analysis of genes downregulated in Cluster 7 compared to the WT group revealed their involvement in epithelial cell proliferation (GO: 0050673) (Fig. 7F). The differentially expressed genes and their corresponding expression levels are listed in Supplementary Table 1.

Discussion

Previous studies have shown that the LSM protein family comprises RNA-binding proteins essential for RNA metabolism. Tang et al. [26] demonstrated that the Lsm2-8 complex protects the mature 3′ end of the telomerase RNA subunit 1 (TER1) in fission yeast, shielding it from exonucleolytic degradation. This protection enhances telomerase activity, preserves telomere stability, and supports cell division. Telomerase typically exhibits heightened activity in stem cells, germ cells, and tumor cells [27]. Additionally, prior research indicates that Lsm2 gene expression significantly correlates with the onset and prognosis of malignant tumors such as breast cancer, melanoma, and hepatocellular carcinoma [13, 15, 16]. Collectively, these findings underscore the association of Lsm2 with cell proliferation.

COPD is a chronic airway disease often caused by smoking [28]. In this study, we initially stimulated 16HBE cells with CSE and observed an increase in Lsm2 expression in vitro. Long-term exposure to cigarette smoke also resulted in elevated Lsm2 expression in vivo. Furthermore, knocking down Lsm2 in 16HBE cells significantly reduced cell viability in vitro (Fig. 1). These experimental results suggest that Lsm2 is crucial for cell proliferation and may play an important role in the pathogenesis of COPD.

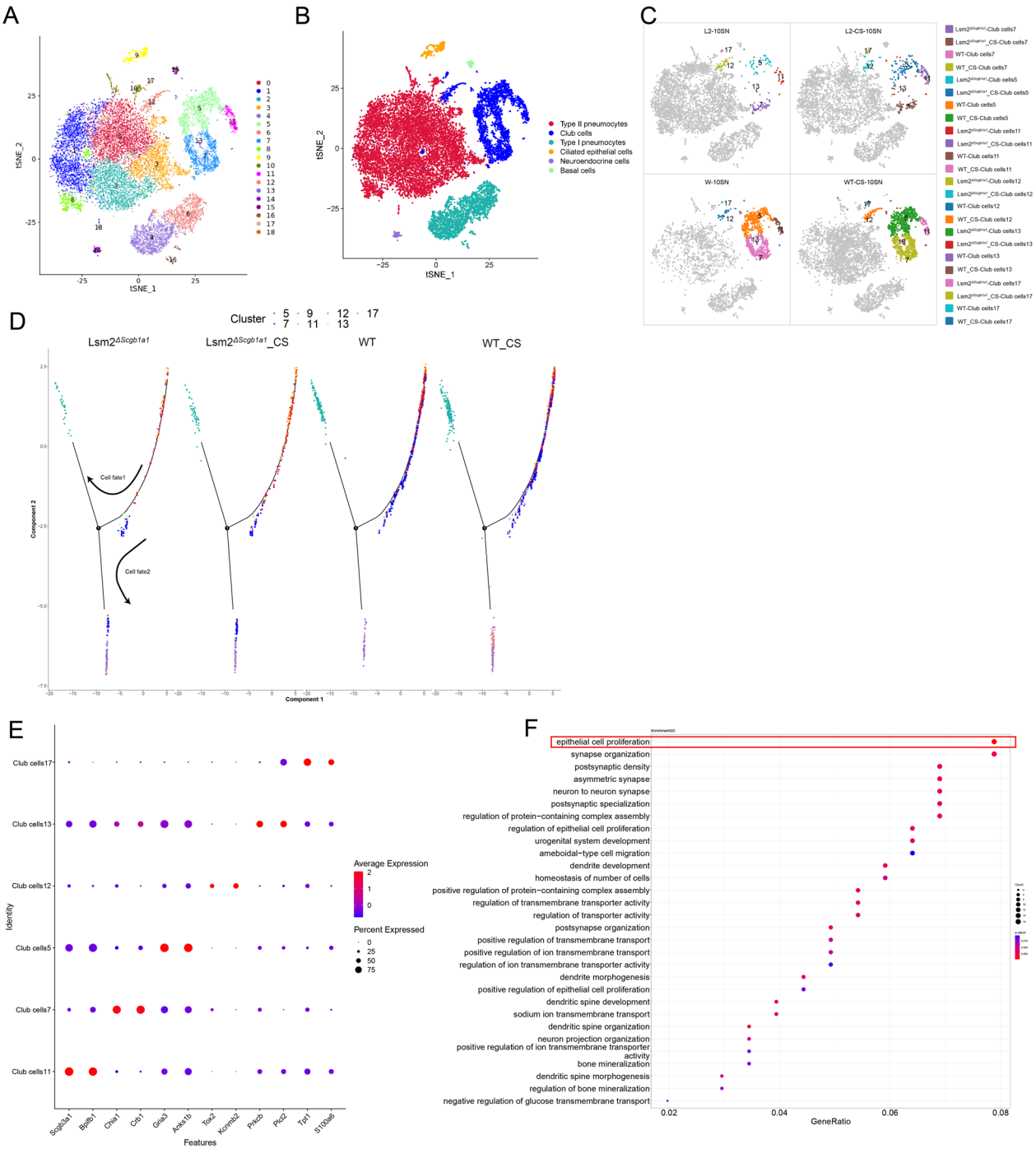

Fig. 7 Chia1^{+}/Crb1^{+} cells play a key role in the transformation of Club cells into ciliated epithelial cells. **A** tSNE visualization of all lung cells showing 18 clusters. **B** tSNE visualization of all epithelial cell types. **C** tSNE visualization of six clusters of Club cells in WT, WT_CS, Lsm2$^{\Delta Scgb1a1}$, and Lsm2$^{\Delta Scgb1a1}$_CS groups. **D** Pseudo-time cell trajectory analysis of the six clusters of Club cells and ciliated epithelial cells. **E** Bubble plots of the marker genes expressed in the six clusters of Club cells. **F** GO analysis of the differentially upregulated genes in the WT group compared to the Lsm2$^{\Delta Scgb1a1}$ group in cluster 7

To investigate the role of Lsm2 in COPD, we developed a conditional Lsm2 knockout mouse (C57BL/6J-Lsm2$^{em\#1(flox)Smoc}$). We first induced lung-specific Lsm2 knockout (Lsm2$^{-/-}$) mice and observed inflammatory cell infiltration, increased secretion of inflammatory factors, and aggravated lung injury (Fig. 2). Since mIHC

staining showed that Lsm2 is mainly expressed in Club cells (Fig. 3), we then generated Club cell-specific Lsm2 knockout mice. We found that Club cell-specific Lsm2 knockout significantly aggravated the infiltration of immune cells, such as macrophages, and increased the secretion of multiple inflammatory factors, including CXCL15, IL-6, and TNF-α (Fig. 3). Macrophage infiltration in the lung creates a more pro-inflammatory environment and causes tissue damage [29]. The high secretion of IL-6, CXCL15, and TNF-α is associated with poor clinical outcomes in COPD [30–32].

RNA-Seq analysis revealed a significant impairment in cilia function in the Lsm2$^{\Delta Scgb1a1}$_CS group compared to the WT_CS group. Subsequent experiments confirmed that this impairment was due to a reduction in the number of ciliated epithelial cells. Ciliated epithelial cells are the predominant epithelial cell type, comprising at least 50% [33]. These cells play a crucial role in airway mucus clearance [9]. Motile cilia (MC) are the primary type in the airway epithelium, forming a natural barrier in the lung bronchial epithelium [8]. In healthy individuals, motile cilia beat at a frequency of 10–14 Hz, clearing inhaled pathogens and particulate matter trapped in the mucus layer from the airways. Typically, a ciliated epithelial cell contains 200–300 cilia [34]. In some patients with COPD, the ciliated epithelial cell structure is altered, resulting in shortened cilia and reduced beating frequency [10, 11]. Cilia dysfunction can exacerbate COPD symptoms. Therefore, we initially hypothesized that Club cell-specific Lsm2 knockout might affect COPD progression by altering cilia structure in ciliated epithelial cells. After cigarette smoke exposure, the WT_CS group did show cilia shortening, structural damage, and a decrease in ciliary oscillation frequency compared to the WT group. However, Club cell-specific Lsm2 knockout exacerbated cigarette smoke-induced cilia shortening without affecting the structure and beating frequency of cilia (Fig. 5A–C).

Immunofluorescence results showed that α-tubulin^{+} cells within the airway epithelium were significantly reduced in both the Lsm2$^{\Delta Scgb1a1}$ and Lsm2$^{\Delta Scgb1a1}$_CS groups compared to the WT and WT_CS groups, respectively (Fig. 5D, E), indicating that Club cell-specific Lsm2 knockout reduces the number of ciliated epithelial cells. Furthermore, single-cell sequencing of lung tissue from mice revealed a significant decrease in the number of Club and ciliated epithelial cells in the Lsm2$^{\Delta Scgb1a1}$ and Lsm2$^{\Delta Scgb1a1}$_CS groups compared to the WT and WT_CS groups, respectively (Fig. 6E, F). Consistent with this, HE staining showed that the airway epithelium in the Lsm2$^{\Delta Scgb1a1}$ and Lsm2$^{\Delta Scgb1a1}$_CS groups is significantly thinner than in the WT and WT_CS groups, respectively (Fig. 3C). The thinning of the airway epithelium may be attributed to the loss of Club and ciliated epithelial cells. These results suggest that Club cell-specific Lsm2 knockout promotes COPD progression by reducing the number of Club and ciliated epithelial cells.

Ciliated epithelial cells require replenishment by a stem cell population [35]. Lineage labeling studies have demonstrated that in bronchioles, both during postnatal growth and adult homeostasis, Club cells possess the capability of self-renewal and differentiation into ciliated epithelial cells [24]. Specifically, in adult bronchioles, almost all renewal of ciliated epithelial cells originates from Club cells [24, 36], which are known for their heterogeneity [37]. Given that functional ciliated epithelial cells were still present in the lungs of mice in the Lsm2$^{\Delta Scgb1a1}$ and Lsm2$^{\Delta Scgb1a1}$_CS groups, it suggests that Lsm2 may not affect all subtypes of Club cells uniformly. To better delineate which Club cell subpopulations are primarily influenced by Lsm2, we further subgrouped the Club cells.

Pseudotime analysis simulates the cell differentiation process. Leveraging the known differentiation relationship between Club cells and ciliated epithelial cells [4, 38], we conducted developmental trajectory analysis on six subpopulations of Club cells and ciliated epithelial cells. We found that the developmental trajectory of cluster 7 of Club cells in the Lsm2$^{\Delta Scgb1a1}$ and Lsm2$^{\Delta Scgb1a1}$_CS groups significantly diverged from that in the WT and WT_CS groups, respectively (Fig. 7D). Cluster 7 of Club cells consists of Chia1^{+}/Crb1^{+} cells. *Bacillus circulans* WL-12 chitinase A1 (Chia1) is an antimicrobial-related protein. Previous studies have shown reduced expression of Chia1 in lung tissue of mice with coal pneumoconiosis compared to normal mice [39]. Crumbs cell polarity complex component 1 gene (Crb1) is highly associated with retinal development and long-term retinal integrity [40]. The high expression of Chia1 and Crb1 in Club cells cluster 7 suggests that the function of this cluster may be related to proliferation and antimicrobial activity. Therefore, we propose that Lsm2 knockout in Club cells leads to a reduction in club cells, specifically inhibits the transdifferentiation of Club cell cluster 7 (Chia1^{+}/Crb1^{+}) into ciliated epithelial cells, ultimately leading to a reduction in the number of ciliated epithelial cells.

In summary, our experimental results demonstrate several key findings: Lsm2 is primarily expressed in Club cells, and exposure to cigarette smoke increases Lsm2 expression. Knockdown of Lsm2 impedes the proliferation of Club cells. Specifically, Club cell-specific knockout of Lsm2 diminishes the population of Club cells, particularly those characterized by Chia1^{+}/Crb1^{+} expression. Consequently, this reduction in Club cells leads to

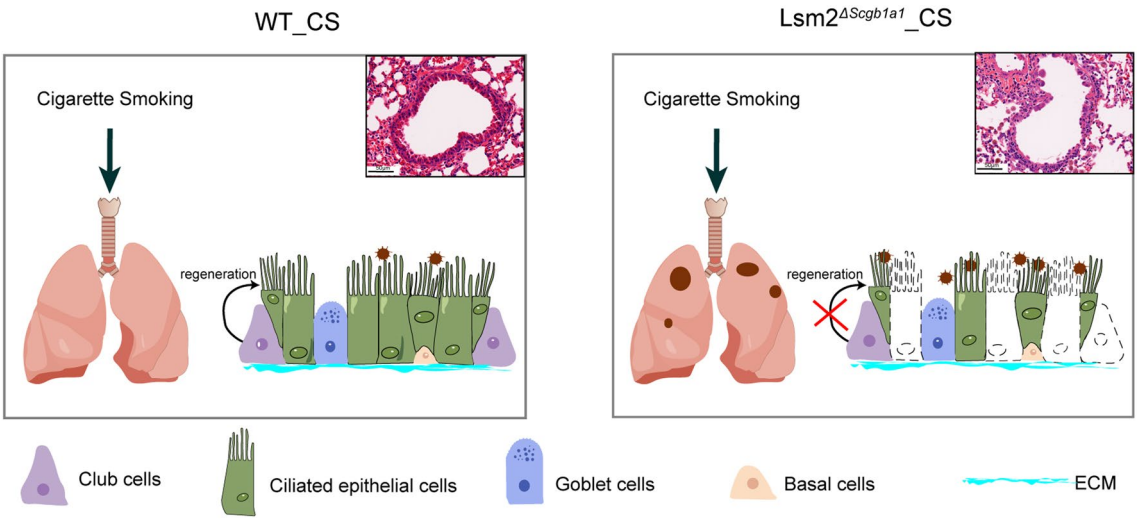

Fig. 8 Lsm2 regulates the progression of COPD by influencing the differentiation of Club cells into ciliated epithelial cells

a decrease in ciliated epithelial cells, rendering the lungs more vulnerable to cigarette smoke and expediting the progression of COPD (Fig. 8).

Conclusion

In this study, we elucidated the protective role of Lsm2 in COPD. Club cell-specific Lsm2 knockout reduced the proliferation of Club cells and disrupted their differentiation into ciliated epithelial cells. Consequently, the number of ciliated epithelial cells decreased, exacerbating lung injury and inflammation induced by cigarette smoke exposure. This aggravated COPD progression and led to a deterioration in lung function.

Abbreviations

COPD	Chronic obstructive pulmonary disease
CC10	Club cell 10 kDa secretory protein
CS	Cigarette smoking
WT	Wild-type
CSE	Cigarette smoke extract
mIHC	Multiplexed immunohistochemistry
ELISA	Enzyme-linked immunosorbent assay
BALF	Bronchoalveolar lavage fluid
IF	Immunofluorescence
SEM	Scanning electron microscopy
TEM	Transmission electron microscopy
NC	Negative control
MAST	Mean alveolar septal thickness
WBC	White blood cell

Supplementary Information

The online version contains supplementary material available at https://doi.org/10.1186/s12931-025-03126-8.

Supplementary Material 1. Figure 1. (A) Multiplexed immunohistochemistry (mIHC) was performed to analyze KRT5 and LSM2 expression (n = 3 biological replicates). (B)The percent of $CC10^+$/Total cells, $FOXJ1^+$/Total cells, and $KRT5^+$/Total cells. (C) $FOXJ1^+LSM2^+$/Total cells (n = 3 biological replicates). *p < 0.05; **p < 0.01.

Supplementary Material 2. Figure 2. Club cell-specific Lsm2 knockout exacerbated cigarette smoke (CS)-induced secretion of inflammatory factors. (A) Luminex assays measuring the levels of IL-6, G-CSF, MIP-1α, MCP-1, CXCL1, and IL-17A in bronchoalveolar lavage fluid (BALF). *p < 0.05; **p < 0.01.

Supplementary Material 3. Figure 3. Club cell-specific Lsm2 knockout induces defects in ciliated epithelial cells. (A) The heatmap of differentially expressed genes between WT_CS group and $Lsm2^{\Delta Scgb1a1}$_CS group. (B) Gene Ontology (GO) enrichment analysis of the downregulated genes in the $Lsm2^{\Delta Scgb1a1}$_CS group compared to the WT_CS group. (C) Relative expression levels of genes involved in cilium assembly, organization, and movement.

Supplementary Material 4. Figure 4. Cellular composition of $CD45^-$ cells. (A) tSNE visualization of $CD45^-$ cells in the WT, WT_CS, $Lsm2^{\Delta Scgb1a1}$, and $Lsm2^{\Delta Scgb1a1}$_CS groups. (B) The number and percentage of the major cell types.

Supplementary Material 5. Figure 5. Club cell-specific Lsm2 knockout decreased the number of Club cells and ciliated epithelial cells. (A) tNSE visualization of all clusters and the distribution of all cells across the four groups. (B) Gene Ontology (GO) analysis of differential genes of ciliated epithelial cells between the WT group and the $Lsm2^{\Delta Scgb1a1}$ group. (C) GO analysis of differential genes of ciliated epithelial cells between the WT_CS group and the $Lsm2^{\Delta Scgb1a1}$_CS group.

Supplementary Material 6. Table 1. The differentially downregulated genes in Club-cells7_ $Lsm2^{\Delta Scgb1a1}$ compared with Club-cells7_WT group, associated with the Gene Ontology term GO: 0050673.

Author contributions

JZ, QLZ, and YS conceived the project and designed the experiments. WSZ, LXH, LDH, WJP, YL, WBT, HQ, SYW, JS, and YLS conducted the experiments and data analysis, and they are listed in order of their workload. JZ, QLZ, and YS wrote the manuscript and all authors contributed to editing.

Funding

This work was supported by the National Natural Science Foundation of China (82070045, 82270040, 82470069), National Key Research and Development Program of China (2023YFC3504300, 2022YFA0806200), Shanghai Municipal Science and Technology Major Project (ZD2021CY001), Science

and Technology Commission of Shanghai Municipality (20DZ2261200, 21DZ2200600, 20DZ2254400, 20Z11901004, 20Z11901000), Shanghai Municipal Key Clinical Specialty (shslczdzk02201), Shanghai Pudong Hospital and the Discipline Construction Promoting Project of Shanghai Pudong Hospital (Zdzk2020-11), Shanghai Jinshan Municipal Health Commission (JSZK2019A01, GWV-10.1-XK26).

Availability of data and materials

All data used or analyzed in this study are available from the corresponding author. The corresponding authors of this study may provide you with the data used or analyzed in this work upon your request.

Declarations

Ethics approval and consent to participate

All animal experiments were approved by the Animal Care and Use Committee of Zhongshan Hospital, Fudan University (No.2023-298).

Competing interests

The authors declare no competing interests.

Received: 22 September 2024 Accepted: 28 January 2025
Published online: 28 February 2025

References

1. Agustí A, Celli BR, Criner GJ, et al. Global initiative for chronic obstructive lung disease 2023 report: GOLD executive summary. Eur Respir J. 2023;61(4):2300239.
2. Agustí A, Melén E, Demeo DL, et al. Pathogenesis of chronic obstructive pulmonary disease: understanding the contributions of gene-environment interactions across the lifespan. Lancet Respir Med. 2022;10(5):512–24.
3. Raby KL, Michaeloudes C, Tonkin J, et al. Mechanisms of airway epithelial injury and abnormal repair in asthma and COPD. Front Immunol. 2023;14:1201658.
4. Reynolds SD, Malkinson AM. Clara cell: progenitor for the bronchiolar epithelium. Int J Biochem Cell Biol. 2010;42(1):1–4.
5. Barnes PJ. Club cells, their secretory protein, and COPD. Chest. 2015;147(6):1447–8.
6. Lomas DA, Silverman EK, Edwards LD, et al. Evaluation of serum CC-16 as a biomarker for COPD in the ECLIPSE cohort. Thorax. 2008;63(12):1058–63.
7. Zhai J, Insel M, Addison KJ, et al. Club cell secretory protein deficiency leads to altered lung function. Am J Respir Crit Care Med. 2019;199(3):302–12.
8. Whitsett JA. Airway epithelial differentiation and mucociliary clearance. Ann Am Thorac Soc. 2018;15(Suppl 3):S143–8.
9. Hill DB, Button B, Rubinstein M, et al. Physiology and pathophysiology of human airway mucus. Physiol Rev. 2022;102(4):1757–836.
10. Yaghi A, Zaman A, Cox G, et al. Ciliary beating is depressed in nasal cilia from chronic obstructive pulmonary disease subjects. Respir Med. 2012;106(8):1139–47.
11. Ancel J, Belgacemi R, Diabasana Z, et al. Impaired ciliary beat frequency and ciliogenesis alteration during airway epithelial cell differentiation in COPD. Diagnostics (Basel). 2021;11(9):1579.
12. Perea-Resa C, Hernández-Verdeja T, López-Cobollo R, et al. LSM proteins provide accurate splicing and decay of selected transcripts to ensure normal Arabidopsis development. Plant Cell. 2012;24(12):4930–47.
13. Sun X, Zhang J, Hu J, et al. LSM2 is associated with a poor prognosis and promotes cell proliferation, migration, and invasion in skin cutaneous melanoma. BMC Med Genomics. 2023;16(1):129.
14. Rahman N, Sun J, Li Z, et al. The cytoplasmic LSm1-7 and nuclear LSm2-8 complexes exert opposite effects on Hepatitis B virus biosynthesis and interferon responses. Front Immunol. 2022;13: 970130.
15. Qin P, Huang H, Wang J, et al. The mechanism of LSM2 in the progression of live hepatocellular carcinoma was analyzed based on bioinformatics. Med Oncol. 2023;40(9):276.
16. Ta HDK, Wang WJ, Phan NN, et al. Potential therapeutic and prognostic values of LSM family genes in breast cancer. Cancers (Basel). 2021;13(19):4902.
17. Hua T, Wang RM, Zhang XC, et al. ZNF76 predicts prognosis and response to platinum chemotherapy in human ovarian cancer. 2021. Biosci Rep. https://doi.org/10.1042/BSR20212026.
18. Pan Y, Liu H, Wang Y, et al. Associations between genetic variants in mRNA splicing-related genes and risk of lung cancer: a pathway-based analysis from published GWASs. Sci Rep. 2017;7:44634.
19. Peng W, Wu Y, Zhang G, et al. GLIPR1 protects against cigarette smoke-induced airway inflammation via PLAU/EGFR signaling. Int J Chron Obstruct Pulmon Dis. 2021;16:2817–32.
20. Zhu W, Han L, Wu Y, et al. Keratin 15 protects against cigarette smoke-induced epithelial mesenchymal transformation by MMP-9. Respir Res. 2023;24(1):297.
21. Han L, Zhu W, Qi H, et al. The cuproptosis-related gene glutaminase promotes alveolar macrophage copper ion accumulation in chronic obstructive pulmonary disease. Int Immunopharmacol. 2024;129: 111585.
22. Wang X, Hao Y, Yin Y, et al. Lianhua qingke preserves mucociliary clearance in rat with acute exacerbation of chronic obstructive pulmonary disease by maintaining ciliated cells proportion and protecting structural integrity and beat function of cilia. Int J Chron Obstruct Pulmon Dis. 2024;19:403–18.
23. Wu Y, Zhu W, Rouzi A, et al. The traditional Chinese patented medicine Qingke Pingchuan granules alleviate acute lung injury by regenerating club cells. Pulm Circ. 2022;12(3): e12138.
24. Rawlins EL, Okubo T, Xue Y, et al. The role of Scgb1a1+ Clara cells in the long-term maintenance and repair of lung airway, but not alveolar, epithelium. Cell Stem Cell. 2009;4(6):525–34.
25. Lafkas D, Shelton A, Chiu C, et al. Therapeutic antibodies reveal Notch control of transdifferentiation in the adult lung. Nature. 2015;528(7580):127–31.
26. Tang W, Kannan R, Blanchette M, et al. Telomerase RNA biogenesis involves sequential binding by Sm and Lsm complexes. Nature. 2012;484(7393):260–4.
27. Collopy LC, Ware TL, Goncalves T, et al. LARP7 family proteins have conserved function in telomerase assembly. Nat Commun. 2018;9(1):557.
28. Gao W, Yuan C, Zhang J, et al. Klotho expression is reduced in COPD airway epithelial cells: effects on inflammation and oxidant injury. Clin Sci (Lond). 2015;129(12):1011–23.
29. Yamasaki K, Eeden SFV. Lung macrophage phenotypes and functional responses: role in the pathogenesis of COPD. Int J Mol Sci. 2018;19(2):582.
30. Rincon M, Irvin CG. Role of IL-6 in asthma and other inflammatory pulmonary diseases. Int J Biol Sci. 2012;8(9):1281–90.
31. Nakamoto K, Watanabe M, Sada M, et al. Pseudomonas aeruginosa-derived flagellin stimulates IL-6 and IL-8 production in human bronchial epithelial cells: a potential mechanism for progression and exacerbation of COPD. Exp Lung Res. 2019;45(8):255–66.
32. Kubysheva N, Boldina M, Eliseeva T, et al. Relationship of serum levels of IL-17, IL-18, TNF-α, and lung function parameters in patients with COPD, asthma-COPD overlap, and bronchial asthma. Mediat Inflamm. 2020;2020:4652898.
33. Wildung M, Herr C, Riedel D, et al. miR449 protects airway regeneration by controlling AURKA/HDAC6-mediated ciliary disassembly. Int J Mol Sci. 2022;23(14):7749.
34. Tilley AE, Walters MS, Shaykhiev R, et al. Cilia dysfunction in lung disease. Annu Rev Physiol. 2015;77:379–406.

35. Zhu L, Jian X, Zhou B, et al. Gut microbiota facilitate chronic spontaneous urticaria. Nat Commun. 2024;15(1):112.
36. Watson JK, Rulands S, Wilkinson AC, et al. Clonal dynamics reveal two distinct populations of basal cells in slow-turnover airway epithelium. Cell Rep. 2015;12(1):90–101.
37. Blackburn JB, Li NF, Bartlett NW, et al. An update in club cell biology and its potential relevance to chronic obstructive pulmonary disease. Am J Physiol Lung Cell Mol Physiol. 2023;324(5):L652–65.
38. Liu Q, Liu K, Cui G, et al. Lung regeneration by multipotent stem cells residing at the bronchioalveolar-duct junction. Nat Genet. 2019;51(4):728–38.
39. Mu M, Li B, Zou Y, et al. Coal dust exposure triggers heterogeneity of transcriptional profiles in mouse pneumoconiosis and Vitamin D remedies. Part Fibre Toxicol. 2022;19(1):7.
40. Rodriguez-Martinez AC, Higgins BE, Tailor-Hamblin V, et al. Foveal hypoplasia in CRB1-related retinopathies. Int J Mol Sci. 2023;24(18):13932.

Publisher's Note